

## Conference paper

Fajun Zhang\*, Felix Roosen-Runge, Andrea Sauter, Marcell Wolf, Robert M. J. Jacobs and Frank Schreiber

# Reentrant condensation, liquid–liquid phase separation and crystallization in protein solutions induced by multivalent metal ions<sup>1</sup>

**Abstract:** We briefly summarize the recent progress in tuning protein interactions as well as phase behavior in protein solutions using multivalent metal ions. We focus on the influence of control parameters and the mechanism of reentrant condensation, the metastable liquid–liquid phase separation and classical vs. non-classical pathways of protein crystallization.

**Keywords:** charge inversion; liquid–liquid phase separation; multivalent salts; protein crystallization; protein interactions; reentrant condensation; zeta-potential.

<sup>1</sup>A collection of invited papers based on presentations at the 33<sup>rd</sup> International Conference on Solution Chemistry (ICSC-33), Kyoto, Japan, 7–12 July 2013.

\*Corresponding author: **Fajun Zhang**, Institut für Angewandte Physik, Universität Tübingen, 72076 Tübingen, Germany, e-mail: fajun.zhang@uni-tuebingen.de

**Felix Roosen-Runge, Andrea Sauter, Marcell Wolf and Frank Schreiber:** Institut für Angewandte Physik, Universität Tübingen, 72076 Tübingen, Germany

**Robert M. J. Jacobs:** Department of Chemistry, Chemistry Research Laboratory, Mansfield Road, University of Oxford, Oxford, OX1 3TA, UK

## Introduction

Interactions of biological macromolecules in aqueous solution are generally complex and depend on a number of environmental parameters including concentration, valence of salt ions, pH, and temperature. These complex interactions lead to a very rich phase diagram that is crucial to our understanding of protein crystallization [1–3], protein condensation-related diseases [1–7], as well as the phase behavior of the cytoplasm in the cell [8–10]. This research field stands where physics and biology must meet. In particular, despite the importance of protein crystallization, our understanding of the physical mechanisms underlying this process is still limited.

Electrostatic interactions are ubiquitous in colloidal, polyelectrolyte, and biological systems, which determine, inter alia, their stability, phase behavior, gene storage and replication of DNA, and the specific interactions of enzymes in vivo [11–13]. Increased interest in this field in the last few decades is in part due to the like-charge attraction observed in various systems of soft matter [14–16]. Theoretical studies and computer simulations have revealed that the electrostatic correlations of multivalent ions can lead to macroion aggregation [17–23]. A phase diagram with a phase separation region, i.e., molecular aggregates around the isoelectric point of the macroion with a subsequent restabilization, and redissolution upon further increasing salt concentration, called reentrant condensation, was predicted [20]. Reentrant phase transitions in multicomponent liquid mixtures have been intensively studied (see review [24]). Reentrant condensation phenomena of polyelectrolyte and DNA in the presence of multivalent counterions are typical examples [17, 25–39].

Proteins are a special type of polyelectrolytes. In contrast to DNA or conventional colloidal systems, both positive and negative charges coexist simultaneously on the surface. Generally, a more complex and more heterogeneous charge pattern prevails, giving rise to significant differences in the interactions. Moreover,

globular proteins exhibit a different shape compared to DNA and conventional colloids. The complex surface charge pattern together with various other interactions, such as hydrophobic interaction and hydration, make the phase behavior of protein solutions more complex [2, 4]. This complicates the theory immensely, and therefore a general description for the reentrant condensation of proteins has yet to be found. Understanding the mechanisms of these protein condensation-related phenomena (crystallization, diseases, and phase transition in cell) strongly depend on the progress in the quantitative characterization of protein interactions under various conditions. While the development of biochemistry provides structural information on the proteins involved in degenerative condensation effects, it is still a long way from understanding structure to fully understanding the nature and mechanism of self-organization processes. A comprehensive understanding leading to the ability to tune protein interactions in solution and alter their phase behavior is essential in order to move forward.

In the last few years, we have studied the effect of charges in protein solutions on both static [16, 40–47] and dynamic behavior [48–51]. Metal ions play a very important role in the function of biological systems. In recent years, trivalent metal ions have been used for fast determination of 3D protein structure, contrast agents in magnetic resonance imaging, and biological labeling. In particular, the paramagnetism of the lanthanide ions offers outstanding opportunities for protein structure determination by NMR spectroscopy [52]. The work summarized here will focus on experimental findings and general concepts and will show that these trivalent metal ions provide an efficient way to tune interactions in protein solutions. One application is the optimization of the conditions for obtaining high-quality protein single crystals for structural biology.

## Reentrant condensation in protein solutions

Reentrant condensation (RC) (Fig. 1) discussed in this paper describes a type of phase behavior in solutions of proteins, DNA, polyelectrolytes, or colloids in the presence of multivalent ions. The corresponding phase diagram such as shown in Fig. 1 contains a phase separation region in between two critical salt concentrations. The first protein–salt system observed experimentally with RC behavior was bovine serum albumin (BSA) in the presence of yttrium chloride ( $\text{YCl}_3$ ) [16]. The experimental observation of BSA with  $\text{YCl}_3$  shows that for a given protein concentration, with increasing salt concentrations, the solution becomes turbid above a critical salt concentration,  $c^*$ . Upon further increasing the salt concentration, the condensed phase is gradually redissolved and the solution becomes clear again above  $c^{**}$ . This observation is further confirmed by the transmission measurement of a series of samples at a constant protein concentration as a function of

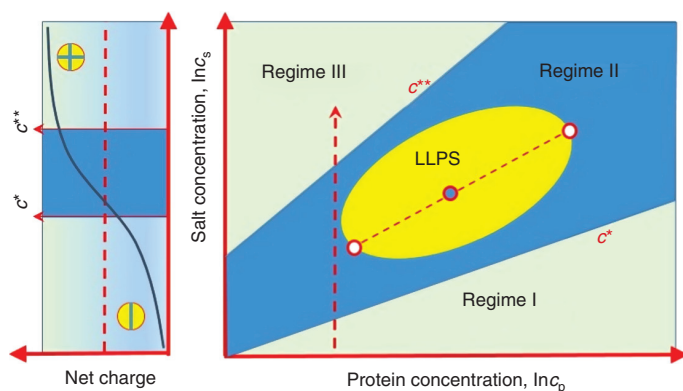


**Fig. 1** Scheme for phase behavior of protein solutions in the presence of trivalent salts. Two critical salt concentrations,  $c^*$  and  $c^{**}$ , divide the isothermal ( $c_s$ ,  $c_p$ ) plane into three regimes that correspond to a reentrant condensation (RC) phase behavior. Within the condensed regime, LLPS occurs in a closed area (yellow ellipsoid). The dashed line corresponds to a tie-line of a pair of solutions after LLPS. Note the protein and salt concentration is given on a logarithmic scale. The charge state of the protein along the dashed arrow is further depicted in the left panel: initially, negatively charged proteins undergo a charge inversion with increasing  $c_s$ .

salt concentration. The evolution of transmission intensity clearly shows a fairly abrupt phase separation approaching  $c^*$  and a subsequent increase of intensity (reentrant condensation) upon further increasing the salt concentration. In addition, computer simulations of the surface charge of BSA as a function of Y(III) concentration also suggest that the surface-exposed side chains of BSA undergo an effective charge inversion over the Y(III) concentration range considered in our experiments, which will obviously modulate the electrostatic interactions. Both  $c^*$  and  $c^{**}$  show in a broad concentration range an approximately linear relationship with respect to the protein concentration,  $c_p$ . The linear relationship for  $c^*$  can be understood by assuming a near-quantitative binding of the ions to the exposed acidic side chains. In this simple model, the exposed side chains are increasingly saturated with trivalent ions binding to them. With this, the number of ions condensed on the surface of a protein for protein condensation and redissolution can be determined from the phase diagram [16, 45].

Further experiments using a number of proteins, such as human serum albumin (HSA),  $\beta$ -lactoglobulin (BLG), ovalbumin, and lysozyme and different multivalent salts including  $\text{LaCl}_3$ ,  $\text{FeCl}_3$ ,  $\text{AlCl}_3$ , and spermine chloride ( $\text{SpeCl}_4$ ) have further clarified the picture. Firstly, the trivalent metal salts cause RC for all proteins tested except lysozyme. Secondly, lysozyme does not show RC with any salt. Thirdly,  $\text{SpeCl}_4$ , a very efficient condensation agent for DNA and polyelectrolytes [25], does not induce RC for protein solutions. This may be simply due to the low charge density, i.e., the charges are so widely spread that they effectively act as singly charged counterions and hence bind nonspecifically. It is worth noting that  $\text{LaCl}_3$  exhibits a phase diagram very similar to  $\text{YCl}_3$ , but different from  $\text{FeCl}_3$  and  $\text{AlCl}_3$ . Proteins with  $\text{FeCl}_3$  and  $\text{AlCl}_3$  exhibit a very narrow condensed regime (in comparison to  $\text{YCl}_3$ ). This behavior is due to the hydrolysis of  $\text{Fe(III)}$  and  $\text{Al(III)}$ , resulting in a lower pH of the solution [40, 45].

We have demonstrated, using spectroscopic techniques, that the secondary structures of the proteins are conserved in the reentrant regime in the presence of multivalent metal ions. Fourier transform infrared spectroscopy (FTIR) measurements indicate that the amide I and amide II bands of the proteins do not change upon mixing with trivalent metal ions, and circular dichroism (CD) spectroscopy measurements show that the CD spectra in the range of 200–250 nm for protein solutions with various salt concentrations overlap with that without salt addition. These two techniques both show that the protein secondary structure is preserved in the presence of metal ions in solution, indicating that the interaction of the metal ions with proteins does not change the native structure of the protein [45, 46].

It is important to realize at this point that the driving mechanism of the reentrant condensation cannot be explained by the Derjaguin–Landau–Verwey–Overbeek (DLVO) theory for colloidal suspensions. Furthermore, although salt effects are key for the observed behavior, the reentrant behavior implies that the conventional approaches for salt-induced protein interactions, namely, the Hofmeister effect or salting-in and salting-out, cannot contribute a consistent picture of the physical mechanisms discussed here.

## Physical mechanism of reentrant condensation phase behavior

The central mechanism during RC is charge inversion, as supported by Monte Carlo simulations initially and further demonstrated experimentally by electrophoretic mobility measurements [16, 40, 45]. Electrophoretic mobility was used to monitor the zeta-potential of proteins as a function of  $c_s$ . Zeta-potential ( $\zeta$ ) distributions for protein solutions as a function of  $c_s$  are narrow and shift continuously to positive surface potential. The plots of  $\zeta$ – $c_s$  for several proteins show a general transition from negative to positive  $\zeta$  values, indicating an effective charge inversion of proteins (Fig. 1, right panel). The comparison between simulations and experimental  $\zeta$  data reveals two main features: The functional form of the  $\zeta$  and the effective protein charge exhibit similar shapes. Both  $\zeta$  and the effective protein charge become zero at about the same salt concentration. The point of zero charge depends on the protein concentration: An increase in protein concentration is accompanied by a shift to a higher salt concentration. This behavior is directly implied in the theoretical concept and is reproduced by simulations. RC is due to an effective charge inversion of proteins with increasing salt concentration. At low salt concentration, proteins are still negatively charged and the long range electro-

static repulsion stabilizes the solution. Increasing the salt concentration, positive metal ions are bound to the protein surface and neutralize the surface charge, until eventually the repulsion vanishes and proteins start to aggregate. Upon further increase of the salt concentration, more and more positive metal ions are bound to the protein surface, and the overall charge on the protein surface becomes positive. A recent study by Kubickova et al. [53] on the overcharging in biological systems also shows the reversal of electrophoretic mobility of aqueous polyaspartate by multivalent cations. The charge reversal as an extreme case of charge compensation is directly observed by capillary electrophoresis for a negatively charged peptide in aqueous solutions of La(III). Atomistic and coarse-grained simulations provide molecular interpretation of this effect, showing that it is largely of electrostatic origin with a minor contribution of chemical specificity of the salt ions.

The RC phase behavior in the presence of Fe(III) and Al(III) show a much narrower phase-separated regime when compared to Y(III). The differences between these salts can be explained by the interplay of pH effects and binding of the multivalent ions. The significant contribution of pH changes caused by the hydrolysis process has to be taken into account to understand the phase behavior. An analytical model has been proposed to take into account ion condensation, metal ion hydrolysis, and interaction with charged amino acid side chains on the protein surface, which reproduces the RC phase behavior established experimentally [40]. Nevertheless, we emphasize that the central effect is the multivalent salt, which can be quantitatively modified by other parameters, such as pH.

We remark that the strongly correlated liquid (SCL) theory has been employed to explain the charge inversion phenomenon in DNA and polyelectrolyte condensation [17]. In this theory a coupling parameter,  $\Gamma$ , is defined which allows systems that can undergo RC ( $\Gamma > 2$ ) to be distinguished from those that cannot ( $\Gamma < 2$ ). While this concept has been very fruitful for certain systems [17, 23], the situation is fundamentally different in the case of proteins. The length scales of ion size, ionic screening, and charge variance on the surface of the protein are all of the same order, rendering not only the validity of mean-field theories but also the applicability of SCL theory questionable. Furthermore, experimental results strongly support the idea of localized binding of the highly charged ions to several discrete spots on the protein surface. In this model, the bound ions cannot freely arrange on the surface. Hence, the average distance of the discrete ions should fail to describe the charge pattern sufficiently well. Nevertheless, it is noted that a naive application of SCL theory to our system can still be performed: Approximating the proteins as uniformly charged spheres with a suitable radius derived from their crystal structures allows a simple computation of the coupling parameter. Such an analysis indeed shows that approximately 95 % of all negatively charged proteins in the PDB would exhibit  $\Gamma > 2$  in this model [45].

## Liquid–liquid phase separation in protein solutions

The RC behavior in protein solutions induced by multivalent metal ions opens a new way to tune the phase behavior of protein solutions. A rich phase behavior has been observed and explored. Within the condensed regime, the condensed protein phase can consist of amorphous clusters, crystals, and, more interestingly, a dense liquid phase.

Temperature-induced liquid–liquid phase separation (LLPS) in aqueous protein solutions (lysozyme in salt water) was first reported by Ishimoto and Tanaka [54]. The concentration-dependent cloud-point temperature was measured as a coexistence curve for liquid–liquid phase equilibrium. The LLPS behavior was further confirmed by the experimental observation of two clear bulk liquid phases separated by a sharp meniscus in lysozyme-water solutions under a variety of conditions. The effects of several parameters, such as ionic strength, the nature of salt, pH, on the LLPS of the lysozyme–water system have been studied [55–59]. Since then, many results were reported of LLPS in protein solutions and further proteins were reported to show LLPS behavior. Benedek and co-workers discovered and studied the LLPS of the lens  $\gamma$ -crystallin family in detail [55, 60–64]. The phase separation of both protein–water binary and ternary mixtures were investigated for a deeper understanding of the formation of cataracts [65]. LLPS of hemoglobin variants (HbS, HbA, and HbC) from normal and sickle cells was studied, which was believed to be closely related to the

pathogenic event for sickle cell anemia [66–68]. LLPS behavior of other proteins such as BPTI [69], glucose isomerase [70] has also been reported. However, fewer than 20 proteins have been studied so far mainly due to the inaccessible temperature range [71, 72]. A mean-field theory of Gibbs free energy has been proposed by Benedek and co-workers to describe the equilibrium conditions for the coexistence of two phases in multicomponent protein–water solution. In the case of ternary solutions of similar proteins, it is possible to analytically describe the coexistence surface, provided the coexistence curves of the binary solutions are known [73].

LLPS in protein solutions can be enhanced by adding nonabsorbing polymer, such as polyethylene (PEG). Adding PEG can significantly enhance the attraction via the depletion mechanism [74, 75]. Kulkarni et al. showed that when the PEG is larger than protein molecules, the concentration fluctuation of PEG strongly affects the interaction between molecules [76]. Systematic studies of the effect of PEG on the LLPS of  $\gamma$ D-crystallin, one of the eye lens proteins, show that the transition temperature increases with both PEG concentration and molecular weight [71]. By this method, the LLPS of  $\gamma$ S-crystallin was successfully observed in the experimental temperature window (–10 to 40°C), which otherwise would occur at –28°C [72]. LLPS of binary protein–water systems may not be directly observable mainly because of the limited temperature window. The increase of the transition temperature is due to the enhanced attraction between protein molecules by adding PEG. The experiments with PEG can be used to adjust the location of the phase boundaries of the binary systems. On the other hand, bio-macromolecular crystallographers have long known that such a liquid phase can be readily observed in many crystallization experiments either prior to the appearance of visible crystals, or directly participating in the crystal growth process [77]. Ray Jr., for example, described protein rich droplets, which were formed when PEG was added to a concentrated protein–salt solution and subsequent crystallization was followed by optical microscopy [78]. It was found that the protein crystals appeared to nucleate at the surface (not within) the droplets, and grow into the protein-poor phase. Importantly, experimental observations also suggest that the liquid–liquid coexistence phases are metastable. Over time, they decay to aggregates, gels, or crystals [56, 58, 66].

Recent studies indicate that LLPS also occurs in several pharmaceutical antibodies [79–85]. Such protein condensation behavior may impact the biological activity, storage stability, and safety of protein therapeutics. Experimental observations indicate that the LLPS of antibody solutions depends on the ionic strength, pH, and type of salts. Wang et al. performed a detailed study on the LLPS of a monoclonal antibody, IgG2 [84]. Interestingly, the phase diagram gives a rather low critical volume fraction of 6.3 % in comparison with the spherical particle solutions, where the critical volume fraction varies from 13 to 23 %. This observation has been attributed to the extended Y-like shape of antibody molecules.

## The physical origin of metastable LLPS in protein and colloidal system

Detailed studies on lysozyme and  $\gamma$ -crystallins lead to the complete phase diagram in the temperature–volume fraction ( $T, \phi$ ) plane [56, 58, 60, 62, 63, 86]. In spite of the differences in size, structure, and biological functions of these proteins, they share a similar phase diagram. The typical features of their phase diagram are that there is no triple point and a metastable liquid–liquid coexistence curve exists below the solubility line (Fig. 2b). The phase behavior is significantly different from that of atomic liquids, such as argon, where the critical point lies above the triple point, indicating the presence of a stable liquid phase. Key ingredients to rationalize the different types of phase behavior and the connection between phase diagrams and the effective interaction potential  $U(r)$  (Fig. 2a) are the range of  $U(r)$  relative to the size of the particles and its depth, which we will discuss in the following.

To explain the LLPS phase behavior as well as the experimentally established phase diagrams of proteins and colloid systems, many theoretical and simulation studies have been performed. Rosenbaum et al. have shown that the crystallization curves for a number of globular protein solutions are similar to those predicted by simulations for a system of hard spheres with a short-range attractive Yukawa potential [86, 87]. Asherie et al. performed a combined analytic and computational study on the phase diagram of colloids

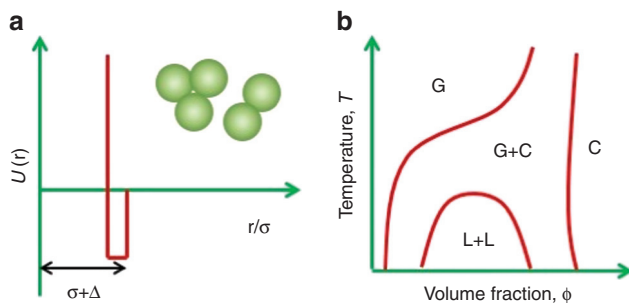


**Fig. 2** (a) A square-well potential existed in protein and colloidal system. When the attractive well-width,  $\Delta$ , is significantly smaller than the diameter of the particle,  $\sigma$ , ( $\Delta/\sigma < 0.25$ ), the phase behavior can be described by the phase diagram (b). The typical feature of the phase diagram is a metastable liquid–liquid coexistence (L+L) below the gas–crystal line (G+C).

[88]. Their study reveals that the interaction range plays a significant role in determining the structure of the phase diagram. A short-range attraction, i.e., the interaction range smaller than  $\sim 25\%$  of the diameter of particles, corresponds to the existence of the meta-stable LLPS in protein and colloid systems. Simulations and theoretical studies also support that a short-range attraction leads to the metastable LLPS [89, 90]. By comparing existing protein crystallization data with knowledge of a model colloid–polymer mixture, where the attraction range as well as strength between colloids can be tuned by varying the molecular weight and concentration of nonabsorbing polymer, Poon suggested a hidden gas–liquid bimodal inside the equilibrium fluid–crystal region of the phase diagram [75]. It is now well accepted that the phase behavior of colloid–polymer mixtures and of protein solutions can be interpreted using a simple model of hard sphere with short-range attraction (Fig. 2a). While such a model qualitatively describes the generic phase diagram, it fails to explain the fact that the model predicts the LLPS in the metastable regime below the curve of dynamical arrest. To solve this problem, Noro et al. proposed that additional long-range attraction may exist in these systems. Such attractions can shift the liquid–liquid critical point out of the gel region, and that may play an important role in protein crystallization [91].

In addition to the spherically symmetric short-range attraction that accounts for the metastable LLPS in the colloidal systems, theoretical and numerical studies on a patchy model suggest that LLPS can also occur by reducing the number of sticky sites [92–95]. The patchy model describes particles decorated on the surface by a predefined number of attractive sticky sites. Interestingly, the phase diagram of patchy colloidal particles shows that the critical point can shift to very low volume fractions with reducing the number of sticky sites. While for colloids with spherically symmetric attraction increasing the range of the attractive potential shifts the critical point to a lower volume fraction [92, 94, 95], this shift occurs in patchy particle systems by reducing the number of patches since the attraction can be saturated at lower volume fractions.

## Liquid–liquid phase separation in protein solutions induced by multivalent metal ions

A metastable LLPS in protein aqueous solution induced by multivalent metal ions at room temperature has been demonstrated in our lab [41]. As shown in Fig. 1, LLPS occurs within a closed area (yellow ellipsoid area) in the condensed regime. For example, HSA, which is a medium-size globular protein very abundant in blood with a molecular weight of 67 kDa, shows LLPS in the presence of  $\text{YCl}_3$ . The sample solution prepared at the condensed regime II is initially turbid. Closer examination by optical microscopy reveals tiny droplets of the protein-rich phase suspended in solution. They can merge and grow, indicating a LLPS. A similar LLPS induced by  $\text{YCl}_3$  is also observed in BSA and  $\beta$ -lactoglobulin solutions [44]. Thus, LLPS can be considered to be a rather universal phenomenon for negatively charged proteins in the presence of trivalent salts.

The partitioning of both salt and protein into two coexisting phases can be determined by X-ray and UV light absorption. In Fig. 1, the pairs of coexisting phases connected by a dashed tie-line define the coexistence region (yellow ellipsoid area) where the LLPS occurs in the  $c_p \sim c_s$  plane within Regime II. The condensed

phase of Regime II outside the LLPS is populated with protein clusters in the low  $c_p$  region or gel in the high  $c_p$  region. It was observed that over long times, the dense liquid phase eventually becomes gel-like and crystals can grow from the dilute phase. This observation suggests the metastability of the coexistence liquid phases, i.e., the free energy of the dense liquid phase is lower than that of the initial solution, whereas it is higher than that of the solid state. The metastability of the LLPS induced by multivalent counterions is similar to the thermally driven LLPS in concentrated protein solutions, such as lysozyme and  $\gamma$ -crystallins. Further studies using small-angle X-ray scattering (SAXS) reveal that the structure factor provides direct evidence for a short-range attraction, which leads to the metastability of the LLPS. A physical mechanism based on the reduced second virial coefficient has been proposed as an indicator for LLPS. In general, theory on the effective one-component system predicts that  $B_2/B_2^{\text{HS}} < 1.5$  is required for LLPS (where  $B_2^{\text{HS}}$  is the excluded volume contribution from a hard sphere) [96–99]. This criterion has been tested in several systems, including hard spheres and mixtures of hard sphere with polymers. The effective interactions in HSA-YCl<sub>3</sub> systems near the boundary of LLPS have been determined by SAXS. Using a square-well potential (Fig. 2a), the  $B_2$  values are obtained, which fit to the theoretical prediction [41].

## Protein crystallization: classical vs. non-classical pathway

The rich phase behavior of protein solution in the presence of multivalent metal ions and the physical understanding based on colloidal theory provide a consistent framework in predicting and optimizing conditions for protein crystallization.

The classical nucleation theory (CNT) describes the free energy cost,  $\Delta G$ , for forming a nucleus of radius  $R$ :  $\Delta G = (4/3)\pi R^3 \rho \Delta\mu + 4\pi R^2 \gamma$ , where  $\rho$  is the number density of the crystal,  $\gamma$  is the crystal–liquid interfacial free energy, and  $\Delta\mu = \mu_c - \mu_l$  is the difference in chemical potential of the crystal and the liquid. The first term expresses the fact that the crystal is more stable than the supersaturated liquid because the sign of  $\Delta\mu$  is negative, and the second term describes the free-energy cost by creating a crystal–liquid interface [3, 100]. The typical free energy landscape (Fig. 3a) shows one energy barrier in between the supersaturated solution and the final crystalline state. While the CNT is widely used to describe various first-order phase transition phenomena, the following limitations become important when applied to more complex systems, such as proteins [101]. CNT predicts the critical nucleus as a spherical droplet with a sharp interface. However, using confocal microscopy, Gasser et al. have observed elliptical nuclei [102]. Yau and Vekilov observed a quasi-planar nucleus in apoferritin crystallization [103]. Furthermore, the size dependence of the surface free energy is neglected in the CNT, which leads to a large discrepancy between simulations and experiment [100]. Recent progress in protein and colloid crystallization as well as biomineralization has shown non-classical features in the early stage of nucleation [104, 105]. While the CNT predicts that the solute molecules reversibly

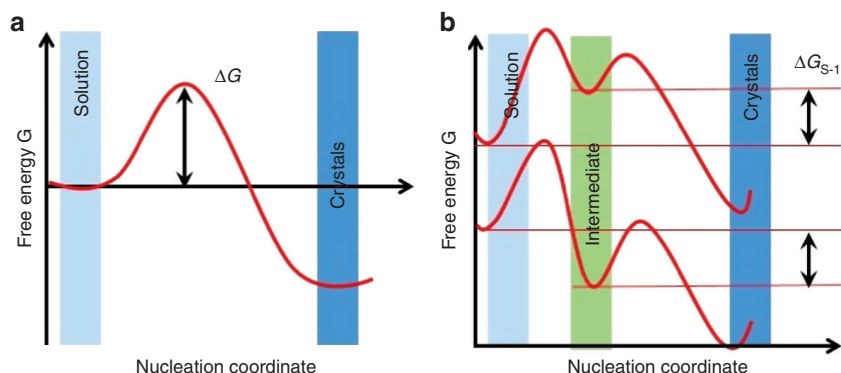


**Fig. 3** Free energy landscape of classical (a) vs. non-classical pathway (b) of nucleation.  $\Delta G_{S-1}$  in (b) represents the free energy difference between the intermediate state and the initial supersaturated solution. Figure 3B is adapted and modified from ref. [111].

aggregate in the supersaturated solution and form nuclei with the exact density and structure of the crystals in the final stage, the non-classical pathway suggests an intermediate phase (clusters or dense liquid phase) to exist in between the initial solution and the final crystalline state [106]. The free energy landscapes of the non-classical pathway show an additional free energy minimum (Fig. 3b) corresponding to the intermediate phase. If the free energy of the intermediate phase is higher than that of the initial solution (top curve in Fig. 3b), it is unstable with respect to the initial solution and the intermediate phase exists as mesoscopic clusters. If the free energy of the intermediate phase is lower than that of the initial solution (bottom curve in Fig. 3b), then the metastable phase can be a dense liquid phase [105].

A “two-step” growth model related to the short-range attraction in protein and colloid systems was first predicted in theory by ten Wolde and Frenkel in 1997 [90]. As shown in Fig. 2b, such systems have a metastable LLPS that alters both the equilibrium phase diagram and the crystal nucleation behavior. When approaching the metastable critical point, the critical nucleus first forms highly disordered, liquid-like droplets that eventually turn into crystalline material [90]. Theoretical considerations also suggest that the density fluctuation in protein or colloidal solutions could enhance nucleation events near the metastable liquid–liquid coexistence curve [56, 89, 107–111]. Separation of order parameters is the key point for the non-classical pathway of protein crystallization. The two-order parameters, density, and structure do not necessarily develop simultaneously.

The two-step mechanism of nucleation has been experimentally observed for several proteins under certain conditions. Galkin and Vekilov performed a systematic study on the kinetics of homogeneous nucleation of lysozyme crystals [57, 111, 112]. This mechanism suggests that the nucleation rate can be controlled either by shifting the phase transition boundary, or by facilitating the structure fluctuation within a dense liquid phase [111]. This two-step crystallization has been reported for small molecules, such as amino acid, calcium carbonate [113], polymers [114, 115], and DNA-functionalized nanoparticles [116]. The two-step mechanism following a metastable LLPS suggests that the nucleation occurs within the dense liquid phase instead of the dilute phase [90, 105, 108]. Because the surface free energy at the interface between the crystal and the solution is significantly higher than at the interface between the crystal and the dense liquid, the barrier for nucleation of crystals from the solution would be much higher. This would lead to much slower nucleation of crystals directly from the solution than inside the dense liquid. While indeed some experimental observations are consistent with this prediction, e.g., for glucose isomerase and hemoglobin [67, 70], other observations show that crystallization prefers to start either at the interface or in the dilute phase [117]. While this has been often attributed to the high viscosity or gelation of the dense liquid phase, a clear understanding of the exact role of precursor structures such as protein clusters and the dense liquid phase is still missing.

## Protein crystallization in the presence of multivalent metal ions

Understanding of protein crystallization is still a challenge: on the one hand, crystal structure determination of macromolecules is often hampered by the lack of crystals suitable for diffraction experiments. Much effort has been employed for optimizing conditions for growing high-quality protein single crystals. On the other hand, the early stage of crystallization, i.e., the nucleation process, is still not well understood. Instead of following the predications of the CNT, the crystal growth of proteins often follows non-classical pathways with an intermediate metastable phase transition as discussed above.

Based on the RC phase behavior, a protocol has been established to crystallize acidic proteins in the presence of yttrium chloride. For example, bovine  $\beta$ -lactoglobulin also exhibits the RC phase behavior with yttrium chloride. The crystallization condition can be further adjusted by temperature. Crystal growth strongly depends on the position in the phase diagram, and the best crystals grow near the phase transition boundaries. It was found that near  $c^*$ , crystal growth follows the classical pathway, i.e., nucleation occurs from the homogeneous supersaturated solution followed by the growth. Near  $c^{**}$ , the solution becomes turbid quickly after quenching to the crystallization temperature. After some time, tiny droplets or aggregates could be observed depending on the initial protein concentration. After that, crystals start to form and grow throughout the sample. Therefore, near  $c^{**}$  we have a typical “two-step” growth process.

The high-quality crystals have been analyzed using X-ray diffraction. The yttrium ions are not only used to engineer the crystallization, but are an integral part of the crystal lattice and can therefore be used to solve the phase problem using anomalous dispersion methods [44]. The structural analysis demonstrates the specific binding of yttrium ions to surface-exposed glutamate and aspartate side chains of different molecules in the crystal lattice. By bridging molecules in this manner, contacts between molecules are formed that enable the formation of a stable crystal lattice [44].

The two-step mechanism of BLG in solution with  $YCl_3$  using SAXS reveals a non-negligible effect of clustering [43]. The protein clusters observed show interesting features with respect to crystallization, which make them suitable as building blocks for crystal formation. Firstly, the clusters have a precrystalline structure, since the cation binding sites represent specific interaction patches. These imprint a favorable structure, as suggested by the SAXS scattering curves of the clusters being simulated well using the clusters created from the crystal structure. Secondly, clusters seem to have an internal flexibility, as evidenced by the pronounced monomer–monomer correlation peak in larger clusters. This flexibility enables local reorientation within the clusters, rendering the precrystalline structure of clusters to be an ideal building block for crystallization, since the enthalpy cost of nucleation via local reorientation is much lower than for a hypothetical nucleation directly from a dimer in solution. Thirdly, the cluster size and its distribution varies throughout the phase diagram; in particular, the clusters grow when the solution conditions approaches the coexistence region. Large precrystalline clusters can serve as the precursor (stabilized nuclei) for further crystal growth, as recently observed in various systems [118–121].

## Conclusions and outlook

Using trivalent metal ions, we discovered the reentrant condensation in protein solutions, which might be the normal behavior for acidic proteins. An analytical model has been developed for charge regulation by taking into account ion condensation, metal ion hydrolysis, and interaction with charged amino acid side chains on the protein surface. Moreover, within the condensed regime, protein solutions can undergo metastable liquid–liquid phase separation, clustering, and protein crystallization, which further demonstrates the possibility to tune the interactions in protein solutions using charge. Furthermore, the application of this framework on protein crystallization have shown that the tunable phase behavior can be used to optimize the conditions for growth of high-quality protein single crystals, which can potentially be applied to all acidic proteins. Systematic studies on the nucleation and crystal growth kinetics under various conditions provide deep insight into the classical and non-classical pathways for protein crystallization, such as a two-step crystallization via a metastable LLPS. The effect of tunable phase behavior in protein solutions using metal ions has potentially far-reaching consequences for a broad range of issues from protein crystallization to protein condensation-related diseases and the structural organization in living cells. It is worth noting that the development of this field is fast. New observations, such as clustering, gelation, or arrested phase separation in protein solutions and more complex phase behavior in cells, all point future research towards the understanding of more complex system in the cell, where multicomponents interact with each other and phase separation leads to structural organization. Using multivalent charges as a control parameter, we are beginning to understand how the fundamental rules of molecular interactions at the atomic length scale propagate and control the structural formation, but there are still many open questions.

**Acknowledgments:** We greatly acknowledge valuable discussions with Prof. R. Roth, Prof. M. Oettel (University of Tübingen), Dr. G. Zocher, Prof. T. Stehle (IFIB, University of Tübingen), Dr. M. Skoda (ISIS, UK), Prof. O. Kohlbacher (Center for Bioinformatics, University of Tübingen), and Dr. T. Narayanan, Dr. M. Sztucki (ESRF, Grenoble, France). We also acknowledge the contributions of many students: M. Hennig, L. Ianessili, B. Heck, F. Zanini, E. Jordan, S. Leibfarth, D. Soraruf, A. Gallice, M. Grimaldo, S. Barsaume, M. Braun, O. Matsarskaia, S. Da Vela. We are grateful for financial support from Deutsche Forschungsgemeinschaft (DFG).

## References

- [1] S. D. Durbin, G. Feher. *Annu. Rev. Phys. Chem.* **47**, 171 (1996).
- [2] R. Piazza. *Curr. Opin. Colloid Interf. Sci.* **8**, 515 (2004).
- [3] V. J. Anderson, H. N. W. Lekkerkerker. *Nature* **416**, 811 (2002).
- [4] R. Piazza. *Curr. Opin. Colloid Interf. Sci.* **5**, 38 (2000).
- [5] A. Tardieu, A. Le Verge, M. Malfois, F. Bonneté, S. Finet, M. Riès-Kautt, L. Belloni. *J. Cryst. Growth* **196**, 193 (1999).
- [6] A. Stradner, G. Foffi, N. Dorsaz, G. Thurston, P. Schurtenberger. *Phys. Rev. Lett.* **99**, 198103 (2007).
- [7] J. D. Gunton, A. Shirayev, D. L. Pagan. *Protein Condensation: Kinetic Pathways to Crystallization and Disease*, Cambridge University Press, New York (2007).
- [8] L. L. Goff, T. Lecuit. *Science* **324**, 1654 (2009).
- [9] C. P. Brangwynne, C. R. Eckmann, D. S. Courson, A. Rybarska, C. Hoege, J. Gharakhani, F. Jülicher, A. A. Hyman. *Science* **324**, 1729 (2009).
- [10] P. Li, S. Banjade, H.-C. Cheng, S. Kim, B. Chen, L. Guo, M. Llaguno, J. V. Hollingsworth, D. S. King, S. F. Banani, P. S. Russo, Q.-X. Jiang, B. T. Nixon, M. K. Rosen. *Nature* **483**, 336 (2012).
- [11] L. Belloni. *J. Phys.: Cond. Matter* **12**, R549 (2000).
- [12] Y. Levin. *Rep. Prog. Phys.* **65**, 1577 (2002).
- [13] G. S. Manning. *Physica A* **231**, 236 (1996).
- [14] T. E. Angelini, H. Liang, W. Wriggers, G. C. L. Wong. *Proc. Natl. Acad. Sci. USA* **100**, 8634 (2003).
- [15] A. E. Larsen, D. G. Grier. *Nature* **385**, 230 (1997).
- [16] F. Zhang, M. W. A. Skoda, R. M. J. Jacobs, S. Zorn, R. A. Martin, C. M. Martin, G. F. Clark, S. Weggler, A. Hildebrandt, O. Kohlbacher, F. Schreiber. *Phys. Rev. Lett.* **101**, 148101 (2008).
- [17] A. Y. Grosberg, T. T. Nguyen, B. I. Shklovskii. *Rev. Mod. Phys.* **74**, 329 (2002).
- [18] P. Linse, V. Lobaskin. *Phys. Rev. Lett.* **83**, 4208 (1999).
- [19] P. Linse, V. Lobaskin. *J. Chem. Phys.* **112**, 3917 (2000).
- [20] V. Lobaskin, K. Qamhieh. *J. Phys. Chem. B* **107**, 8022 (2003).
- [21] M. Lund, B. Jönsson. *Biophys. J.* **85**, 2940 (2003).
- [22] J. Wu, D. Bratko, J. M. Prausnitz. *Proc. Natl. Acad. Sci. USA* **95**, 15169 (1998).
- [23] I. Rouzina, V. A. Bloomfield. *J. Phys. Chem.* **100**, 9977 (1996).
- [24] T. Narayanan, A. Kumar. *Physics Reports* **249**, 135 (1994).
- [25] V. A. Bloomfield. *Curr. Opin. Struct. Biol.* **6**, 334 (1996).
- [26] M. Saminathan, T. Antony, A. Shirahata, L. H. Sigal, T. Thomas, T. J. Thomas. *Biochemistry* **38**, 3821 (1999).
- [27] Y. Burak, G. Ariel, D. Andelman. *Biophys. J.* **85**, 2100 (2003).
- [28] J. Yang, D. C. Rau. *Biophys. J.* **89**, 1932 (2005).
- [29] P. Y. Hsiao. *J. Chem. Phys.* **124**, 044904 (2006).
- [30] T. T. Nguyen, I. Rouzina, B. I. Shklovskii. *J. Chem. Phys.* **112**, 2562 (2000).
- [31] M. Olvera de la Cruz, L. Belloni, M. Delsanti, J. P. Dalbiez, O. Spalla, M. Drifford. *J. Chem. Phys.* **103**, 5781 (1995).
- [32] F. J. Solís, M. Olvera de la Cruz. *J. Chem. Phys.* **112**, 2030 (2000).
- [33] B. I. Shklovskii. *Phys. Rev. E* **60**, 5802 (1999).
- [34] J. C. Butler, T. Angelini, J. X. Tang, G. C. L. Wong. *Phys. Rev. Lett.* **91**, 028301 (2003).
- [35] B. I. Shklovskii. *Phys. Rev. Lett.* **82**, 3268 (1999).
- [36] W. M. Gelbart, R. F. Bruinsma, P. A. Pincus, V. A. Parsegian. *Phys. Today* **53**, 38 (2002).
- [37] A. A. Kornyshev, D. J. Lee, S. Leikin, A. Wynveen. *Rev. Mod. Phys.* **79**, 943 (2007).
- [38] Y. Murayama, Y. Sakamaki, M. Sano. *Phys. Rev. Lett.* **90**, 018102 (2003).
- [39] K. Besteman, K. Van Eijk, S. G. Lemay. *Nat. Phys.* **3**, 641 (2007).
- [40] F. Roosen-Runge, B. S. Heck, F. Zhang, O. Kohlbacher, F. Schreiber. *J. Phys. Chem. B* **117**, 5777 (2013).
- [41] F. Zhang, R. Roth, M. Wolf, F. Roosen-Runge, M. W. A. Skoda, R. M. J. Jacobs, M. Sztucki, F. Schreiber. *Soft Matter* **8**, 1313 (2012).
- [42] F. Zhang, F. Roosen-Runge, M. W. A. Skoda, R. M. J. Jacobs, M. Wolf, P. Callow, H. Frielinghaus, V. Pipich, S. Prévost, F. Schreiber. *Phys. Chem. Chem. Phys.* **14**, 2483 (2012).
- [43] F. Zhang, F. Roosen-Runge, A. Sauter, R. Roth, M. W. A. Skoda, R. M. J. Jacobs, M. Sztucki, F. Schreiber. *Faraday Discuss.* **159**, 313 (2012).
- [44] F. Zhang, G. Zocher, A. Sauter, T. Stehle, F. Schreiber. *J. Appl. Crystallogr.* **44**, 755 (2011).
- [45] F. Zhang, S. Weggler, M. Ziller, L. Ianeselli, B. S. Heck, A. Hildebrandt, O. Kohlbacher, M. W. A. Skoda, R. M. J. Jacobs, F. Schreiber. *Proteins: Struct., Funct., Bioinformatics* **78**, 3450 (2010).
- [46] L. Ianeselli, F. Zhang, M. W. A. Skoda, R. M. J. Jacobs, R. A. Martin, S. Callow, S. Prévost, F. Schreiber. *J. Phys. Chem. B* **114**, 3776 (2010).
- [47] F. Zhang, M. W. A. Skoda, R. M. J. Jacobs, R. A. Martin, C. M. Martin, F. Schreiber. *J. Phys. Chem. B* **111**, 251 (2007).
- [48] M. Hennig, F. Roosen-Runge, F. Zhang, S. Zorn, M. W. A. Skoda, R. M. J. Jacobs, T. Seydel, F. Schreiber. *Soft Matter* **8**, 1628 (2012).

- [49] M. Heinen, F. Zanini, F. Roosen-Runge, D. Fedunová, F. Zhang, M. Hennig, T. Seydel, R. Schweins, M. Sztucki, M. Antalík, F. Schreiber, G. Nägele. *Soft Matter* **8**, 1404 (2012).
- [50] F. Roosen-Runge, M. Hennig, F. Zhang, R. M. J. Jacobs, M. Sztucki, H. Schober, T. Seydel, F. Schreiber. *Proc. Natl. Acad. Sci. USA* **108**, 11815 (2011).
- [51] F. Roosen-Runge, M. Hennig, T. Seydel, F. Zhang, M. W. A. Skoda, S. Zorn, R. M. J. Jacobs, M. Maccarini, P. Fouquet, F. Schreiber. *Biochim. Biophys. Acta* **1804**, 68 (2010).
- [52] E. A. Permyakov. *Metalloproteomics*. John Wiley, Hoboken, NJ (2009).
- [53] A. Kubíčková, T. Křížek, P. Coufal, M. Vazdar, E. Wernersson, J. Heyda, P. Jungwirth. *Phys. Rev. Lett.* **108**, 186101 (2012).
- [54] C. Ishimoto, T. Tanaka. *Phys. Rev. Lett.* **39**, 474 (1977).
- [55] V. G. Taratuta, A. Holschbach, G. M. Thurston, D. Blankschtein, G. B. Benedek. *J. Phys. Chem.* **94**, 2140 (1990).
- [56] M. Muschol, F. Rosenberger. *J. Chem. Phys.* **107**, 1953 (1997).
- [57] O. Galkin, P. G. Vekilov. *Proc. Natl. Acad. Sci. USA* **97**, 6277 (2000).
- [58] D. N. Petsev, X. Wu, O. Galkin, P. G. Vekilov. *J. Phys. Chem. B* **107**, 3921 (2003).
- [59] M. L. Broide, T. M. Tominc, M. D. Saxowsky. *Phys. Rev. E* **53**, 6325 (1996).
- [60] J. A. Thomson, P. Schurtenberger, G. M. Thurston, G. B. Benedek. *Proc. Natl. Acad. Sci. USA* **84**, 7079 (1987).
- [61] P. Schurtenberger, R. A. Chamberlin, G. M. Thurston, J. A. Thomson, G. B. Benedek. *Phys. Rev. Lett.* **63**, 2064 (1989).
- [62] M. L. Broide, C. R. Berland, J. Pande, O. Ogun, G. B. Benedek. *Proc. Natl. Acad. Sci. USA* **88**, 5660 (1991).
- [63] C. R. Berland, G. M. Thurston, M. Kondo, M. L. Vroide, J. Pande, O. Ogun, G. B. Benedek. *Proc. Natl. Acad. Sci. USA* **89**, 1214 (1992).
- [64] O. Annunziata, A. Pande, J. Pande, O. Ogun, N. H. Lubsen, G. B. Benedek. *Biochemistry* **44**, 1316 (2005).
- [65] C. Liu, N. Asherie, A. Lomakin, J. Pande, O. Ogun, G. B. Benedek. *Proc. Natl. Acad. Sci. USA* **93**, 377 (1996).
- [66] Q. Chen, P. G. Vekilov, R. L. Nagel, R. E. Hirsch. *Biophys. J.* **86**, 1702 (2004).
- [67] O. Galkin, K. Chen, R. L. Nagel, R. E. Hirsch, P. G. Vekilov. *Proc. Natl. Acad. Sci. USA* **99**, 8479 (2002).
- [68] P. L. San Biagio, M. U. Palma. *Biophys. J.* **60**, 508 (1991).
- [69] S. Grouazel, J. Perez, J. P. Astier, F. Bonneté, S. Veessler. *Acta Crystallogr., Sect. D* **58**, 1560 (2002).
- [70] D. Vivares, E. W. Kaler, A. M. Lenhoff. *Acta Crystallogr., Sect. D* **61**, 819 (2005).
- [71] O. Annunziata, N. Asherie, A. Lomakin, J. Pande, O. Ogun, G. B. Benedek. *Proc. Natl. Acad. Sci. USA* **99**, 14165 (2002).
- [72] O. Annunziata, O. Ogun, G. B. Benedek. *Proc. Natl. Acad. Sci. USA* **100**, 970 (2003).
- [73] C. Liu, A. Lomakin, G. M. Thurston, D. Hayden, A. Pande, J. Pande, O. Ogun, N. Asherie, G. B. Benedek. *J. Phys. Chem.* **99**, 454 (1995).
- [74] S. Asakura, F. Oosawa. *J. Chem. Phys.* **22**, 1255 (1954).
- [75] W. C. K. Poon. *J. Phys.: Cond. Matter* **14**, R859 (2002).
- [76] A. M. Kulkarni, A. P. Chatterjee, K. S. Schweizer, C. F. Zukoski. *Phys. Rev. Lett.* **83**, 4554 (1999).
- [77] Y. G. Kuznetsov, A. J. Malkin, A. Mcpherson. *J. Cryst. Growth* **232**, 30 (2001).
- [78] W. J. Ray Jr., C. E. Bracker. *J. Cryst. Growth* **76**, 562 (1986).
- [79] S. Chen, H. Lau, Y. Brodsky, G. R. Kleemann, R. F. Latypov. *Protein Sci.* **19**, 1191 (2010).
- [80] B. D. Mason, J. Zhang-van Enk, L. Zhang, R. L. Remmele Jr, J. Zhang. *Biophys. J.* **99**, 3792 (2010).
- [81] H. Nishi, M. Miyajima, H. Nakagami, M. Noda, S. Uchiyama, K. Fukui. *Pharm. Res.* **27**, 1348 (2010).
- [82] R. A. Lewus, P. A. Darcy, A. M. Lenhoff, S. I. Sandler. *Biotechnol. Prog.* **27**, 280 (2011).
- [83] E. Trilisky, R. Gillespie, T. D. Osslund, S. Vunnum. *Biotechnol. Prog.* **27**, 1054 (2011).
- [84] Y. Wang, A. Lomakin, R. F. Latypov, G. B. Benedek. *Proc. Natl. Acad. Sci. USA* **108**, 16606 (2011).
- [85] Y. Wang, A. Lomakin, T. Hideshima, J. P. Laubach, O. Ogun, P. G. Richardson, N. C. Munshi, K. C. Anderson, G. B. Benedek. *Proc. Natl. Acad. Sci. USA* **109**, 13359 (2012).
- [86] D. Rosenbaum, P. C. Zamora, C. F. Zukoski. *Phys. Rev. Lett.* **76**, 150 (1996).
- [87] M. H. J. Hagen, D. Frenkel. *J. Chem. Phys.* **101**, 4093 (1994).
- [88] N. Asherie, A. Lomakin, G. B. Benedek. *Phys. Rev. Lett.* **77**, 4832 (1996).
- [89] J. F. Lutsko, G. Nicolis. *Phys. Rev. Lett.* **96**, 046102 (2006).
- [90] P. R. ten Wolde, D. Frenkel. *Science* **277**, 1975 (1997).
- [91] M. G. Noro, N. Kern, D. Frenkel. *Europhys. Lett.* **48**, 332 (1999).
- [92] E. Bianchi, J. Largo, P. Tartaglia, E. Zaccarelli, F. Sciortino. *Phys. Rev. Lett.* **97**, 168301 (2006).
- [93] B. Ruzicka, E. Zaccarelli, L. Zulian, R. Angelini, M. Sztucki, A. Moussaïd, T. Narayanan, F. Sciortino. *Nat. Mater.* **10**, 56 (2011).
- [94] F. Sciortino, E. Zaccarelli. *Curr. Opin. Solid State Mater. Sci.* **15**, 246 (2011).
- [95] G. Jackson, W. G. Chapman, K. E. Gubbins. *Mol. Phys.* **65**, 1 (1988).
- [96] G. A. Vliegthart, H. N. W. Lekkerkerker. *J. Chem. Phys.* **112**, 5364 (2000).
- [97] M. G. Noro, D. Frenkel. *J. Chem. Phys.* **113**, 2941 (2000).
- [98] D. J. Ashton, N. B. Wilding, R. Roth, R. Evans. *Phys. Rev. E* **84**, 061136 (2011).
- [99] R. Roth, R. Evans, A. A. Louis. *Phys. Rev. E* **64**, 051202 (2001).
- [100] S. Auer, D. Frenkel. *Nature* **409**, 1020 (2001).
- [101] D. Erdemir, A. Y. Lee, A. S. Myerson. *Acc. Chem. Res.* **42**, 621 (2009).

- [102] U. Gasser, E. R. Weeks, A. Schofield, P. N. Pusey, D. A. Weitz. *Science* **292**, 258 (2001).
- [103] S. T. Yau, P. G. Vekilov. *Nature* **406**, 494 (2000).
- [104] D. Gebauer, H. Cölfen. *Nano Today* **6**, 564 (2011).
- [105] P. G. Vekilov. *Nanoscale* **2**, 2346 (2010).
- [106] F. C. Meldrum, R. P. Sear. *Science* **322**, 1802 (2008).
- [107] G. Nicolis, C. Nicolis. *Physica A* **323**, 139 (2003).
- [108] V. Talanquer, D. W. Oxtoby. *J. Chem. Phys.* **109**, 223 (1998).
- [109] A. Lomakin, N. Asherie, G. B. Benedek. *Proc. Natl. Acad. Sci. USA* **100**, 10254 (2003).
- [110] D. F. Rosenbaum, C. F. Zukoski. *J. Cryst. Growth* **169**, 752 (1996).
- [111] P. G. Vekilov. *Cryst. Growth Des.* **4**, 671 (2004).
- [112] O. Galkin, P. G. Vekilov. *J. Am. Chem. Soc.* **122**, 156 (2000).
- [113] D. Gebauer, A. Völkel, H. Cölfen. *Science* **322**, 1819 (2008).
- [114] R. H. Gee, N. Lacevic, L. E. Fried. *Nat. Mater.* **5**, 39 (2006).
- [115] P. D. Olmsted, W. C. K. Poon, T. C. B. McLeish, N. J. Terrill, A. J. Ryan. *Phys. Rev. Lett.* **81**, 373 (1998).
- [116] W. Dai, S. K. Kumar, F. W. Starr. *Soft Matter* **6**, 6130 (2010).
- [117] Y. Liu, X. Wang, C. B. Ching. *Cryst. Growth Des.* **10**, 548 (2010).
- [118] A. Navrotsky. *Proc. Natl. Acad. Sci. USA* **101**, 12096 (2004).
- [119] S. Mintova, N. H. Olson, V. Valtchev, T. Bein. *Science* **283**, 958 (1999).
- [120] G. Furrer, B. L. Phillips, K.-U. Ulrich, R. Pöthig, W. H. Casey. *Science* **297**, 2245 (2002).
- [121] J. F. Banfield, S. A. Welch, H. Zhang, T. T. Ebert, R. Lee Penn. *Science* **289**, 751 (2000).